



Yakınsak-Konik Nozulların Giriş ve Çıkış Çaplarının İtme Kuvveti ve Hacimsel Debi Üzerindeki Etkisinin Teorik, Nümerik ve Deneysel İncelemesi

Theoretical, Numerical and Experimental Investigation of the Inlet and Exit Diameter Effect of Convergent-Conical Nozzles on Thrust Force and Volumetric Flow Rate

Berkan Hızarcı^{1*}, **Zeki Kırıl²**

¹ TOFAŞ Türk Otomobil Fabrikası Anonim Şirketi, Ar-Ge, Güç Sistemleri, Bursa, Türkiye

² Dokuz Eylül Üniversitesi, Mühendislik Fakültesi, Makina Mühendisliği Bölümü, Buca, İzmir, 35390, Türkiye

Sorumlu Yazar / Corresponding Author *: berkan.hizarci@tofas.com.tr

Geliş Tarihi / Received: 26.07.2022

Kabul Tarihi / Accepted: 28.12.2022

Araştırma Makalesi/Research Article

DOI:10.21205/deufmd.2023257501

Atıf şekli/ How to cite: HIZARCI, B. , KIRAL, Z.(2023). Yakınsak-Konik Nozulların Giriş ve Çıkış Çaplarının İtme Kuvveti ve Hacimsel Debi Üzerindeki Etkisinin Teorik, Nümerik ve Deneysel İncelemesi. DEUFMD, 25(75), 525-538.

Öz

Yakınsak konik tipi nozulları günlük hayattan roket bilimine kadar her yerde görmek mümkündür. Püskürtme için hava üfleme tabancaları, sıkıştırma için buhar türbinleri, itme üretimi için roketler ve irtifa kontrolü için uydular gibi birçok uygulamada tahrik sisteminin ana parçası olarak kullanılırlar. Bu çalışma, genellikle hava üfleme tabancalarda kullanılan eksenel simetrik yakınsak-konik nozullara odaklanmaktadır. Literatürde, yakınsak-konik nozüller ile ilgili çalışmaların çoğu, Hesaplamalı Akışkanlar Dinamiği (CFD) simülasyonları ile sıkıştırılabilir akış üzerindeki yarım-konik açı etkilerini araştırmaktadır. Literatürde, aynı yarım açya sahip bir nozul için giriş ve çıkış çapı değişiminin etkilerini birden fazla yaklaşımla karşılaştırarak inceleyen bir çalışmaya rastlanmamıştır. Bu nedenle, bu çalışmanın amacı, aynı koni-yarım açısına sahip yakınsak-konik nozüllerin farklı giriş ve çıkış çapları için itme ve hacimsel akış hızındaki değişiklikleri araştırmak ve teorik, sayısal ve deneysel sonuçları karşılaştırmaktır. Bu çalışmada, yakınsak konik nozullerin teorik olarak incelenmesi için yarı-tek boyutlu Euler denklemleri tanımlanmıştır. Ancak bu yaklaşımda viskoz kayıplar gibi birçok önemli özellik ihmal edilmektedir. Aslında, nozul akışları, sıkıştırılabilir etkilerden dolayı şok dalgaları, türbülans ve sınır tabakaları gibi oldukça karmaşık özelliklere sahiptir. Bu nedenle, bu çalışmada nozulun sayısal olarak incelenmesi için Ansys Fluent ile Hesaplamalı Akışkanlar Dinamiği (CFD) simülasyonları yapılmıştır. CFD simülasyonları, yakınsak konik tip nozul akışlarının daha iyi anlaşılmasını ve görselleştirilmesini sağlar. Üçüncü bir yaklaşım için, itme ve hacimsel akış hızı ölçümleri ile deneysel araştırma yapılmıştır. Teorik ve sayısal sonuçlar deneysel sonuçlarla karşılaştırılmış ve deneysel sonuca en yakın olanı bulmak için benzerlik oranları tanımlanmıştır.

Anahtar Kelimeler: Yakınsak Nozul, Çap Etkisi, İtme Kuvveti, Hacimsel Debi, Ansys Fluent

Abstract

It is possible to see convergent-conical nozzles everywhere, from daily life to rocket science. They are utilized as the main part of the propulsion system in many applications such as air blow guns for

spraying, steam turbines for compression, rockets for thrust generation, satellites for altitude control and so on. This study focuses on the axisymmetric convergent-conical nozzles, generally used in air blow guns. In the literature, most of the studies about convergent-conical nozzles investigate the cone-half angle effects on the compressible flow with Computational Fluid Dynamics (CFD) simulations. A study examining the effects of inlet and outlet diameter changes for a nozzle having the same half-angle by comparing more than one approach has not been encountered in the literature. Therefore, this study aims to investigate the changes in thrust and volumetric flow rate for different inlet and exit diameters of convergent-conical nozzles with the same cone-half angle and compare theoretical, numerical, and experimental results. In this study, the quasi-one-dimensional Euler equations are defined for the theoretical investigation of convergent conical nozzles. However, in this approach, many important features such as viscous losses are neglected. Nozzle flows have highly complex features including shock waves, turbulence, and boundary layers due to compressible effects. Thus, CFD simulations are performed with ANSYS Fluent for numerical investigation of the nozzle in this study. CFD simulations provide a better understanding and illustration of convergent-conical nozzle flows. For a third approach, the experimental investigation is conducted for thrust and volumetric flow rate measurements. Theoretical and numerical results are compared with the experimental results and similarity ratios are defined to find the closest to the experimental results.

Keywords: *Convergent Nozzle, Diameter Effect, Thrust Force, Volumetric Flow Rate, ANSYS Fluent*

1. Introduction

A nozzle is a pipe or tube with varying cross-sectional area and is used to control the speed or the direction of a fluid flow [1]. They are extensively utilized in many machines such as rockets, steam turbines, jet engines and in many applications like flow measurement, cleaning, cutting, cooling, coating, moistening, drying, and lubrication. There are three types of nozzles: convergent, divergent and convergent-divergent. A convergent nozzle is a nozzle with a continuously decreasing cross-sectional area from the nozzle inlet to the exit. If the cross-sectional area of the nozzle increases from the nozzle inlet to the exit, it is called a divergent nozzle. The convergent-divergent nozzle consists of using these two nozzles together, the first convergent part, then the divergent part. The convergent nozzles with axisymmetric and conical geometries are of interest to this study because they are the most common nozzles encountered in daily life such as spray nozzles in cleaning applications, jet nozzles in ventilation operations and exhaust nozzles in propulsion systems.

The high-pressure fluid at the nozzle inlet always flows into the low-pressure nozzle exit. Meanwhile, the fluid accelerates as it passes through the decreasing cross-sectional area of the nozzle. The momentum of a fluid whose mass does not change, but whose velocity increases. According to the conservation of momentum, which is a consequence of Newton's 1st law of motion, the momentum gained by the fluid must

be balanced within the system to maintain the total momentum of the system. This balance is achieved by assuming that a force is applied against the direction of the fluid. This force is often called thrust. This thrust force is investigated extensively in the literature [2] since it is encountered in many places in daily life. For example, it is known that the air coming out of the balloon moves the balloon forward. The second example is an air gun or water jet cleaning gun. When using these tools, a thrust is created in the hand and even countered by a reaction force to hold the tool in place. This principle forms the basis of the technology used in rockets today. This study especially focuses on the axisymmetric convergent-conical nozzles, which are generally used in air blow guns. In literature, these nozzles are used as a part of the actuator [3,4]. They are examined by looking at the supply pressure versus flow rate chart in the datasheets. However, there is no information about their thrust in the datasheets. Therefore, in this study, the real convergent-conical nozzles with 3 different inlet and outlet diameters but the same converging angle are investigated for thrust and flow characterization.

The thrust and flow rate are the most important parameters to be considered while designing a pneumatic system including a nozzle. The thrust is related to the force applied to the system due to the compressed flow, and the flow rate is related to the consumption of pneumatic energy. Due to the flow from the nozzle, the thrust depends upon the pressure, mass flow rate,

velocity of the fluid, and the cross-sectional area of the nozzle exit. Therefore, thrust, flow rate and flow contour generated by nozzles change according to nozzle geometry. To date, some studies have been carried out on the analysis of compressible flow through nozzles. While many are concerned with CFD analysis of convergent-divergent nozzles [5,6,7], little courtesy is given to the converging nozzle. In the literature, Thornock and Brown [8] performed an experimental study about the effect of cone-half nozzle angles on the propulsive performance and characteristics of the flow by comparing experimental results with the theoretical solutions. The nozzles of 15°, 25° and 40° cone-half-angle and constant 3.0 in. exit diameter were utilized. Spotts et al. [9] studied numerical simulations on the same nozzles of Thornock and Brown with the help of Metacomp CFD++ software. That study focused on assessing the accuracy of the CFD results in obtaining nozzle performance by compared with the available experimental data of Thornock and Brown [8]. They concluded that the results predicted by the CFD software generally are consistent with the literature data for different nozzle pressure ratios (NPRs). Su and Cheng [10] conducted numerical and experimental research on the convergence angle of the wet sprayer nozzle. They investigated a convergent nozzle with a cone-half angle between 3° and 7° used in a shotcrete operation for the construction of both ground projects and underground projects, such as tunnels, subways, slopes, roadways, etc. Sun et al. [11] studied the influences of the design parameters on the performance of a double serpentine convergent nozzle which looks like an 'S' shape. They compared six different turbulence models to the experimental data of axial thrust to determine the suitable turbulence model for serpentine duct simulations. They found that the SST $K-\omega$ turbulence model is the most suitable for the experimental data of the serpentine convergent nozzle. Kumar et al. [12] performed numerical simulations to visualize the fluid flow and thermal characteristics of a non-axisymmetric convergent nozzle designed based on a curve-fitting approach. In the study, the inlet and exit diameter of the nozzle is constant, but the nozzle angle starts with 18.6855° changes over the nozzle length with 0.03813°. Alam et al. [13] investigated the effect of nozzle geometries on the discharge coefficient. They used cylindrical convergent nozzles, conical convergent nozzles and conical divergent orifices with varying radius of

curvatures, convergent and divergent angles. The convergent angles of the conical nozzles used in the study are 30°, 45°, 60° and 75°. The exit diameter of the all nozzles is constant and 12.7 mm. Payri et al. [14] studied converging nozzles used as diesel direct injection sprays with three different diameters to investigate spray droplet velocity characterization. The main objective of the study was to establish relationships between nozzle geometry and spray dynamics. Three converging nozzles with different inlet and outlet diameters and different converging angles were used in the study. Jiang et al. [15] carried out both experiments and CFD simulations to understand the effect of different converging angles and throat lengths of the conestraight nozzle on internal and external flow patterns. The influence of 10°, 15°, 20° and 25° nozzle converging angles and 0, 4, 8, 12, and 16 mm throat length on the viscous force were examined. Lakdawala et al. [16] investigated jet expansion for hydraulic nozzles produced with different materials such as polymer and stainless steel. These nozzles had the same inlet diameter (40 mm), but different exit diameters (17, 18, 19, 22, and 25 mm). Kubo et al. [17] experimentally investigated the choking phenomenon of a convergent nozzle with a constant inlet diameter (75 mm) and exit diameter (15 mm) followed by a straight pipe of four variable lengths (113, 150, 300 and 450 mm).

From the studies about converging nozzles in the literature, it can be seen that only the effect of converging angles and different nozzle shapes has been investigated so far. However, the effect of different inlet and exit diameters on flow characteristics for the nozzles having the same converging angle has not yet been comprehensively studied. Therefore, the novelty of this study is the using three different methodologies for the investigation of the effect of diameter changes on convergent-conical nozzles flows. The nozzles used in this study have different inlet and outlet diameters but the same cone-half angle. The distinction between nozzles used in this study and the previous literature studies can be seen in Table 1.

Table 1. Comparison of the nozzle geometric properties used in this study and previous studies.

Tablo 1. Bu ve önceki çalışmalarda kullanılan nozul geometrik özelliklerinin karşılaştırılması.

Parameters	This study	[6], [7]	[8]	[10]	[11]	[12] (µm)	[13]	[14]
Inlet radius (r_i)-mm	3-4.5-4.5	73.5	64	6	11	61-83.5	2	20
Exit radius (r_e)-mm	0.75-0.75-0.5	38.1	45	1.8	6.35	53.5-74.5	1	8.5-12.5
Cone half angle (θ)-deg	20-20-20	15-40	3-7	18.6	30-75	2.1-2-1.8	10-25	10-16

The objectives of the study can be summarized as given below:

- Investigation of inlet and exit diameter effect on thrust and flow rate for the convergent conical nozzles having the same cone-half angle.
- The flow characteristics of convergent-conical nozzles are examined by using three different approaches:
 - 1D Euler fluid dynamic equations for compressible flow on nozzles,
 - CFD simulations with Fluent
 - Real experiments.
- Calculating the similarity ratios between the results

2. Theoretical Investigation

The traditional Bernoulli equation may be used to study low-speed gas and liquid flows where the flow has no compressibility effects. However, high-speed gas dynamics may show compressible effects which dominate the gas flow characterization. In the Bernoulli principle, the compressible effects such as the change in density of the fluid is ignored for the low-speed flows. However, enormous changes occur in the density of the fluid in the nozzle flow. Therefore, the mathematical formulation of inviscid compressible nozzle flows is described with quasi-1D Euler equations in this study. The quasi-1D Euler equations are utilized since flow parameters of gas through the nozzle are assumed to change along only nozzle length due to changing cross-section area, as seen in Figure 1. For analysing the 1D nozzle flow, isentropic flow and ideal gas law are assumed, and effects of body forces, viscous stress and heat fluxes are neglected. The governing equations in steady-state conditions are given in Equation (1), where x is the position coordinate along the nozzle axis, A is the cross-section area, ρ is the density of the fluid, V is the velocity in x direction, P is pressure,

h is enthalpy, R is the gas constant, T is the temperature of the fluid, γ is the ratio of specific heats and subscripts 't' stands for total or stagnation conditions.

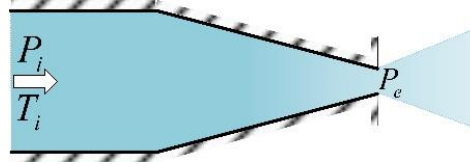


Figure 1. Scheme of the convergent nozzle

Şekil 1. Yakınsak nozulun şeması

$$\left\{ \begin{array}{l} \frac{d}{dx}(\rho VA) = 0 \\ \rho V \frac{dV}{dx} + \frac{dP}{dx} = 0 \\ \frac{d(h + V^2/2)}{dx} = 0 \\ P = \rho RT \\ \frac{P}{P_t} = \left(\frac{T}{T_t}\right)^{\gamma/\gamma-1} \end{array} \right. \quad (1)$$

Equations are mass conservation, momentum conservation, energy conservation, state equation and isentropic relation, respectively. Thermodynamic relations for perfect dry air gas are assumed such as $R = 287.058 \text{ J}/(\text{Kg}\times\text{K})$, $h = C_p T$, $\gamma = C_p/C_v$ where C_v and C_p are specific heat capacity at constant volume and pressure, respectively. At 300 K air, $C_p = 1005 \text{ (Pa}\times\text{m}^3)/(\text{kg}\times\text{K})$, $C_v = 718 \text{ (Pa}\times\text{m}^3)/(\text{kg}\times\text{K})$, and $\gamma = 1.4$. Since the maximum Mach number at the exit of a convergent nozzle can be 1, the nozzle exit pressure is limited with a critical pressure (P^*) whose equation is given in Equation (2).

$$P^* = \left(\frac{2}{\gamma + 1}\right)^{\gamma/\gamma-1} P_t \quad (2)$$

$$\left\{ \begin{array}{l} F = \dot{m} M_e \sqrt{\gamma R T_e} \\ T_e = T_t \left(\frac{P_e}{P_t} \right)^{\gamma/\gamma-1} \\ M_e = \sqrt{\frac{2}{\gamma-1} \left(\left(\frac{P_e}{P_t} \right)^{\gamma/\gamma-1} - 1 \right)} \\ \dot{m} = \sqrt{\frac{\gamma}{R T_t}} P_t \left(1 + \frac{\gamma-1}{2} M_e^2 \right)^{\gamma+1/2-2\gamma} M_e A_e \end{array} \right\} : P_a \geq P^* \text{ (Subsonic flow at nozzle exit)}$$

$$\left\{ \begin{array}{l} F = \dot{m} M_e \sqrt{\gamma R T_e} + (P^* - P_a) A_e \\ T_e = T_t \left(\frac{2}{\gamma+1} \right) \\ M_e = 1 \\ \dot{m} = \sqrt{\frac{\gamma}{R T_t}} P_t \left(\frac{\gamma+1}{2} \right)^{\gamma+1/2-2\gamma} A_e \end{array} \right\} : P_a < P^* \text{ (Sonic flow at nozzle exit)}$$

Two cases, subsonic exit and sonic exit, may appear at the convergent nozzle exit according to the critical pressure, given in Equation 2. Subsonic flow at the nozzle exit appears when ambient pressure (P_a) equals or is more than the critical pressure ($P_a \geq P^*$). For subsonic flow, the exit pressure of the convergent nozzle equals ambient pressure ($P_e = P_a$), where subscripts ‘e’ stands for nozzle exit. When the ambient pressure is less than the critical pressure ($P_a < P^*$), the sonic flow at the convergent nozzle exit appears and the nozzle exit pressure equals the critical pressure ($P_e = P^*$). When Equation (1) is rearranged with the above information, the thrust force, mass flow rate, Mach number and fluid temperature at nozzle exit can be found as in Equation (3) for subsonic and sonic exit [18].

3. Numerical Investigation

Due to compressible flow effects, nozzle flows can have complex features including shock waves and boundary layers. To examine nozzle flows comprehensively, CFD simulations are generally required with three-dimensional flow solvers. In this study, ANSYS Fluent software was utilized to investigate the nozzle flow.

3.1. Nozzle geometry, computational domain and boundary conditions

In this study, three different nozzles named Type 1, 2 and 3 are examined. The geometries of the nozzles are given in Table 2.

Table 2. Geometrical properties of the nozzles.

Table 2. Nozulların geometrik özellikleri.

Parameters	Unit	Type1	Type2	Type3
Inlet radius (r_i)	mm	3	4.5	4.5
Exit radius (r_e)	mm	0.75	0.75	0.5
Cone half angle (θ)	deg	20	20	20
Nozzle length (L)	mm	15	21	21
Cone length (L_c)	mm	6.182	10.3	11
Wall thickness (w)	mm	2	2.5	2.5

From Table 2, the difference between the nozzles is the radius of the nozzle inlet and exit. Therefore, in this study, the effect of nozzle inlet and exit radius on thrust and flow rate have been investigated. Since the nozzles are conical, nozzles are designed as axisymmetric in the CFD simulations. The computational domain of fluid includes both internal and external flow of the nozzle, which can be seen in Figure 2. This domain takes into account the expansion of flow into the atmosphere and provides more accurate behaviour of the fluid flow. The size of the computational domain has been determined as in the study of Yaravintelimath et al. [19]. The boundary conditions determined by examining the study of Elmekawy [20]. are given in Table 3.

Table 3. Boundary conditions.

Tablo 3. Sınır koşulları.

Boundary	Type	Condition
Nozzle inlet	Pressure inlet	Gauge total pressure:121-709kPa,Initial pressure:101 kPa,Total temp:285 K
Outflow	Pressure outlet	Gauge pressure: 101 kPa, Backflow total temperature:300K
Axis	Axis	-
Wall	Wall	No slip, stationary wall

The operating pressure under operating conditions is set to 0 Pa according to the density relationship with the ideal gas law. The geometrical properties of the nozzles are obtained from visual inspection and their datasheets [21].

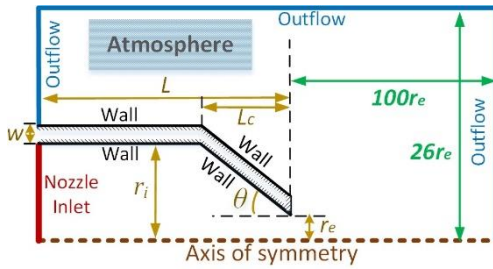


Figure 2. Nozzle dimensions, computational domain and boundary conditions

Şekil 2. Nozul boyutları, hesaplama alanı ve sınır koşulları

3.2. Mesh generation

A high-quality mesh is one of the important factors to ensure accurate and stable results in

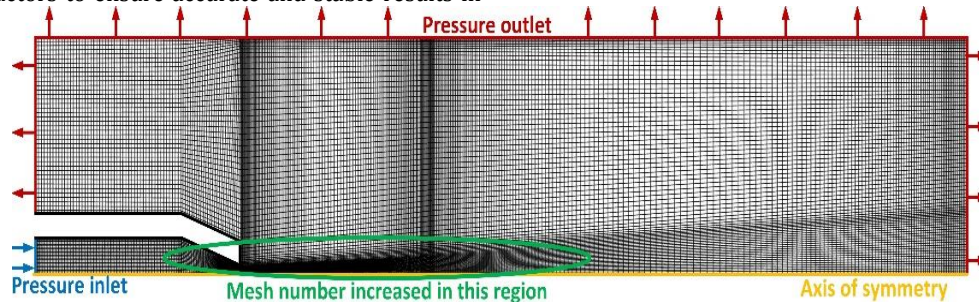


Figure 3. Mesh generation and boundary conditions

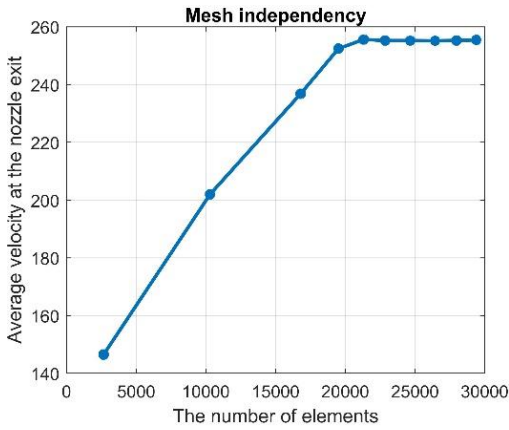
Şekil 3. Ağ oluşumu ve sınır koşulları

CFD analysis. For mesh type, a 2D quadrilateral element with 4 nodes (Quad4) was used in this study. A face meshing was applied to the model as it provides simple and high-quality mesh on approximately rectangular geometry. The edges on the computational domain is divided with edge sizing to get a smaller mesh so that the maximum element size is 0.6 mm for all simulations. The mesh configuration is inspired by the grids of the axisymmetric subsonic jet case of NASA [22]. All mesh configurations are the same for all nozzle types. An example of mesh generation is given in Figure 3. As can be seen in Figure 3, the mesh number has been increased around the nozzle exit where the flow is compressed and expanded.

High and similar mesh quality is important for the reliability of the results gathered from the numerical analyzes. Therefore, the quality of mesh has been determined by mesh metrics. According to [23], skewness and aspect ratio are two important parameters related to mesh quality. The general rule for acceptable mesh is that the maximum skewness should be kept below 0.95, with an average value less than 0.33, and it is best to avoid aspect ratios above 10. The mesh metrics for this study are given in Table 4. As can be understood from Table 4, the quality of the mesh in the analysis is very high and similar for all types. The mesh independency test result is given with the average velocity at the nozzle exit with respect to the number of elements in Figure 4. It can be stated from Figure 4 that the result variations are not significant after 22000 elements. Therefore, the mesh having around 22000 elements can be considered better for less time of simulations. However, in this study, a finer mesh is preferred to get reliable results from all simulations for three types of nozzles.

Table 4. Mesh metrics.**Tablo 4.** Ağ metrikleri.

Parameters	Type1	Type2	Type 3
Nodes	26663	26942	27492
Elements	26144	26382	26924
Skewness (max)	0.2433	0.2451	0.27707
Skewness (avg)	0.0275	0.0286	0.0295
Aspect ratio (max)	7.3049	5.8308	7.4269

**Figure 4.** Mesh independency test result**Şekil 4.** Ağ bağımsızlığı testi sonucu

3.3. Numerical setups

For this study, the governing equations of continuity, momentum, and energy are discretized using the finite volume method, linearized implicitly, and solved by a pressure-based coupled solver with ANSYS Fluent. The steady simulation is conducted in axisymmetric 2D space. In simulations, for the materials of fluid, the air is utilized, an ideal gas is assumed and Sutherland viscosity law is applied for the effect of molecular viscosity on temperature. The default values for C_p (1006.43), and the molecular weight (28.966) are used.

Several researchers have tried various turbulence models for the accurate prediction of flow separation on converging nozzles. In [24], the "Standard" Spalart-Allmaras (SA) and Menter Shear Stress Transport (SST) are examined for turbulence models. In [20], the k-

omega and SST model is preferred for converging nozzles. In [14], SA and SST models are compared for different nozzle types. In this study, the turbulence model is selected as k-omega ($k-\Omega$) and SST due to the successful results presented in [20]. In solution methods, the coupled scheme is chosen and the following options are selected under spatial discretization: least squares cell-based gradient, second-order pressure, second-order upwind density, second-order upwind momentum, second-order upwind turbulent kinetic energy, second-order upwind specific dissipation rate, second order upwind energy according to Elmekawy [20]. The iteration limit is chosen as 1000.

3.4. Simulation results

The simulations are performed for various NPRs from 1.5 to 6.0. NPRs are equal to nozzle inlet pressure divided by ambient (atmosphere) pressure (P_i/P_a). Through NPR, the input pressures of the nozzles are parameterized in the simulations. Air jet flow patterns are illustrated in Figure 5 by the contours of Mach numbers. Mach contours with their reflections with respect to the axis of symmetry are given for NPRs 2, 3, 4 and 6. The average Mach numbers at the nozzle exit and maximum Mach numbers through the flow are provided in Figure 5. Moreover, the mass flow rate values are provided in the same figure. From the results given in Figure 5, maximum Mach numbers and Mach numbers at nozzle exits are approximately the same for all nozzle types and all NPRs. It can be seen from Figure 5 that the jet flow patterns and mass flow rates of Type 1 are very similar to those of Type 2. This indicates that the nozzle inlet diameter has little effect on nozzle flow. However, the Type 3 jet length is shorter for all NPRs than the other two types. Besides, the mass flow rate of Type 3 is less than the other two types for all NPRs. This means that the smaller outlet diameter of the nozzles results in a shorter jet length and less mass flow rate. It is well-known that the maximum Mach number at the convergent nozzle exit can be 1. However, as can be seen in Figure 5, the Mach number increases and becomes more than 1 after the nozzle exit. This phenomenon occurs as the flow suddenly opens to the atmosphere and is exposed to high expansion. Since there is an increase in the flow area, isentropic expansion occurs and that makes the subsonic to supersonic flow after the nozzle exit.

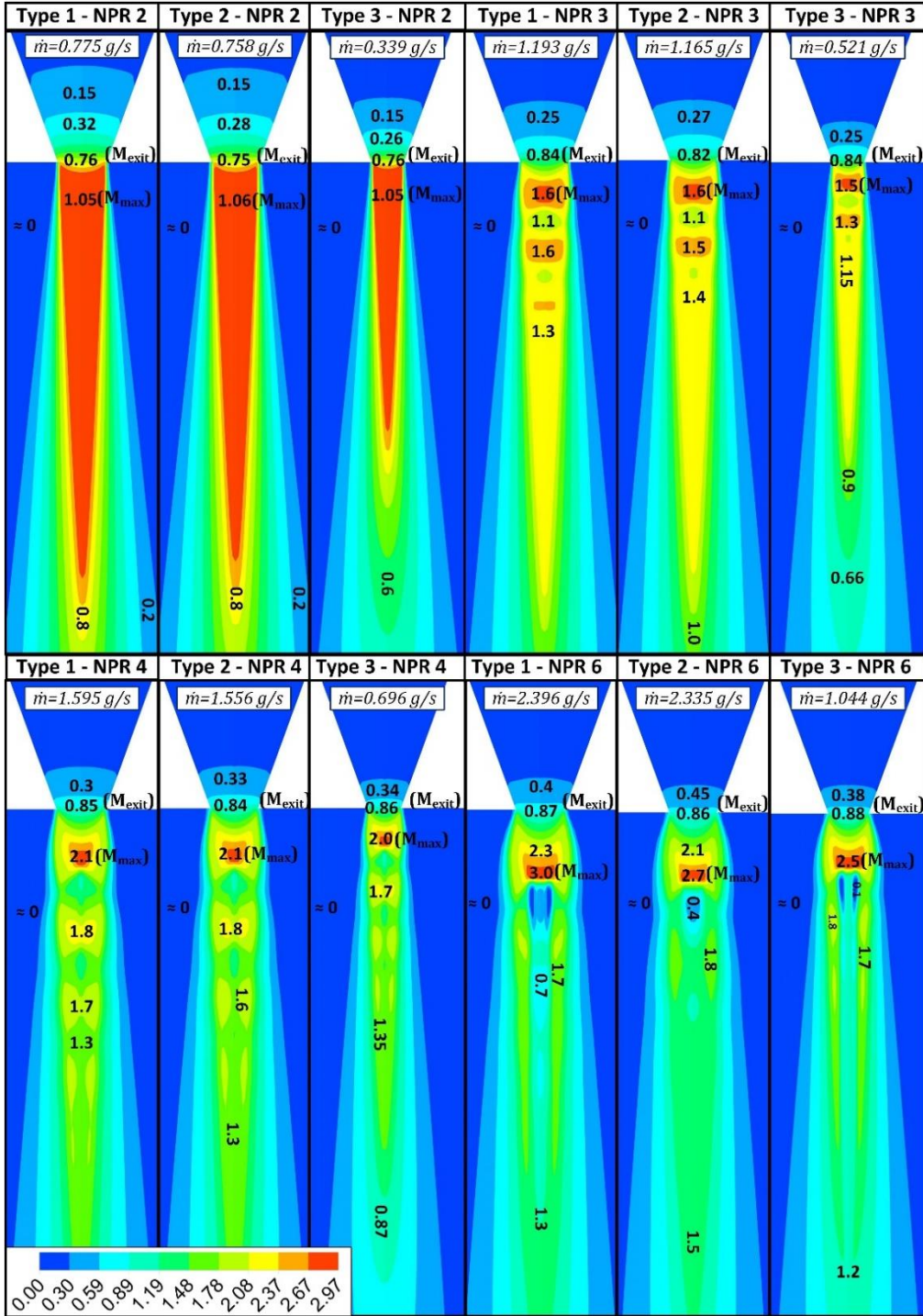


Figure 5. Air jet flow patterns by Mach number contours

Şekil 5. Mach sayısı konturlarına göre hava jeti akış modelleri

4. Experimental Investigation

To compare and verify the results between approaches, the thrust experiments are also conducted. To conduct the experiments, the Type 1, 2 and 3 nozzles whose properties are given in Table 2 were purchased from the SMC Corporation as KN-R01-150, KN-R02-150, and KN-R02-100 product numbers, respectively. These nozzles are shown in Figure 6.



Figure 6. Views of the nozzles in the study

Şekil 6. Çalışmadaki nozulların görünüşleri

The experimental setup for thrust and volumetric flow rate (VFR) measurement can be seen in Figure 7. The experimental setup consists of an air compressor, water separator, air filter, mist separator, electro-pneumatic regulator (EPR), volumetric flow meter, nozzles, air pressure sensor and load cell. The electronic devices used in the experiments in this study and their sensitivity are given in Table 5. The maximum pressure of the air compressor was set to 7 bar. The water separator, air filter and mist separator are used to remove bulk fluid, dust and vapor from the compressed air, respectively. During the experiments, the nozzle inlet pressure is adjusted with the EPR (ITV2050).

Table 5. Electronic devices in the study.

Tablo 5. Çalışmadaki elektronik cihazlar.

Device	Unit	Range	Sensitivity
ITV2050	MPa	0.005-0.9	0.2% F.S.
PFMB7201	L/min	2-200	1.0% F.S.
Load-Cell	N	0-10	0.3% F.S.
Pressure Sensor	MPa	0-1.2	1.5% F.S.

ITV2050, produced by SMC Corporation, controls the air pressure proportional to an input electric signal and allows conducting the experiments for 1.5 to 6.0 NPRs by changing the inlet pressure of the nozzle. The PFMB7201 flow meter, produced by SMC Corporation, is utilized to measure the volumetric flow rate. The nozzles are placed on the load cell to measure the amount of nozzle thrust. The load cell has been used in experiments as a force converter to convert the thrust generated by the nozzles into an electrical signal. When the thrust generated by the nozzle is applied to the load cell, the body of the load cell is slightly deformed. In response to the load-cell body shape changes, the strain gauge on the load-cell also changes shape. This causes an increase in the overall electrical resistance across the strain gauges. The difference in resistance is proportional to the thrust and it is measured as a voltage change. In this way, the thrust is measured from the change in voltage. However, this voltage change is very small, on the order of millivolts, therefore it is amplified for proper measurement by an electronic component (HX711) in this study. The experiments are conducted for all nozzle types under the same operating conditions. First, the pressure at the nozzle inlet is adjusted by the electro-pneumatic regulator (EPR) between 1-6 NPR. It is important to state that even if the desired inlet pressure is set with the EPR, a pressure loss may occur due to the pneumatic pipeline in the experimental setup. Therefore, the pneumatic pressure sensor (DN10) was used nearby the nozzles to measure the correct air pressure at the nozzle inlet. The correct NPR has been calculated with the pressure measured by the pressure sensor. Then, the volumetric flow rate through the pneumatic pipe is measured via the flow meter.

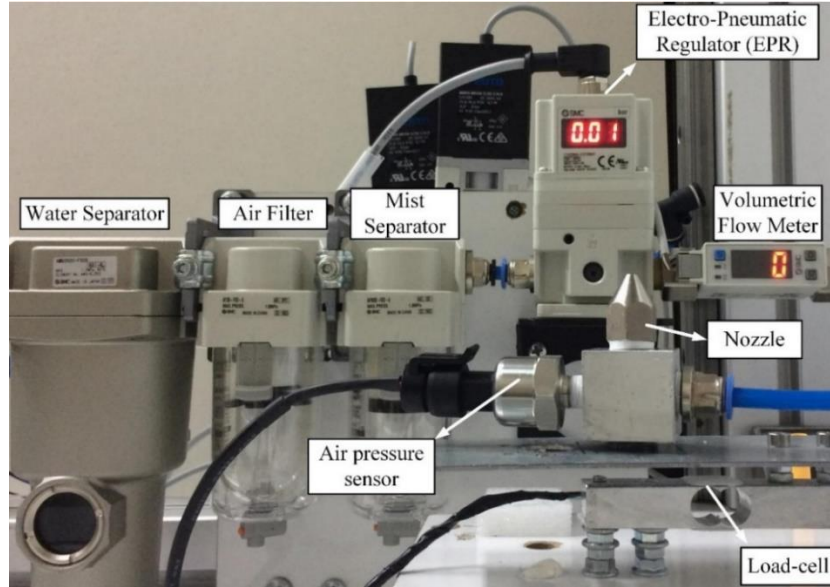


Figure 7. Experimental setup for thrust and volumetric flow rate measurements

Şekil 7. İtme ve hacimsel akış hızı ölçümleri için deney düzeneği

The nozzles are mounted on the load cell as can be seen in Figure 7 to measure thrust changes. The nozzle starts producing thrust after 1 NPR and this thrust is sensed by the load cell as resistance changes on the strain gauges and these changes are measured as analogue voltage changes from the microcontroller. In the experimental part of the study, the thrust and volumetric flow rate according to NPR are

measured and they are compared with the results of the other two approaches.

5. Results

The thrust and volumetric flow rate comparisons between the experiments and the other two approaches are given in Figure 8 (a) and (b), respectively.

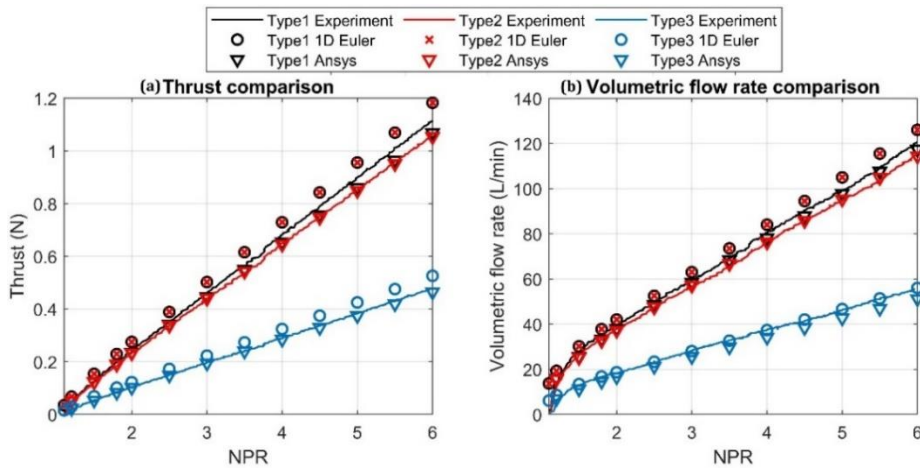


Figure 8. Comparison of the theoretical, numerical and experimental results

Şekil 8. Teorik, sayısal ve deneysel sonuçların karşılaştırılması

According to the experimental thrust results in Figure 8 (a), the Type 1 nozzle has the greatest

thrust and the Type 2 nozzle thrust is very close to the Type 1's thrust. The least thrust value

belongs to the Type 3 nozzle. As a result, it can be stated that although the inlet diameter of nozzles slightly affects thrust and volumetric flow rate, the exit diameter dramatically changes the results. The larger exit diameter provides more flow rate and thrust. From the theoretical results, it is observed that the thrust and volumetric flow rate results of Type 1 and Type 2 are the same. That means the change in inlet radius does not change nozzle thrust and flow rate for theoretical investigation. On the other

hand, the real results show that it is hardly true. Since the large radius causes a large surface area, thus more considerable friction, the larger inlet diameter gives slightly lower results for numerical and experimental approaches. Some of the results with percentage errors are also given in Table 6. As understood from Table 6, the theoretical approach has generally larger errors than the numerical approach. The closer results are provided by ANSYS Fluent for Type 2 and Type 3 nozzles.

Table 6. Errors between the results in percentage.

Tablo 6. Yüzde cinsinden sonuçlar arasındaki hatalar.

Nozzle	NPR	THRUST (N)			VOLUMETRIC FLOW RATE (L/min)		
		Experiment	1D EULER (% Error)	ANSYS (% Error)	Experiment	1D EULER (% Error)	ANSYS (% Error)
Type 1	1.5	0.126	0.154 (22.22%)	0.122 (-3.17%)	27.71	30.13 (8.73%)	25.67 (-7.36%)
	2	0.238	0.275 (15.55%)	0.235 (-1.26%)	39.22	41.99 (7.06%)	37.98 (-3.16%)
	4	0.684	0.729 (6.58%)	0.653 (-4.53%)	80.36	83.98 (4.51%)	78.16 (-2.74%)
	6	1.116	1.183 (6.00%)	1.068 (-4.30%)	120.6	126.1 (4.56%)	117.4 (-2.65%)
Type 2	1.5	0.122	0.154 (26.23%)	0.122 (0.00%)	26.24	30.13 (14.82%)	25.16 (-4.12%)
	2	0.233	0.275 (18.02%)	0.233 (0.00%)	37.75	41.99 (11.23%)	37.16 (-1.56%)
	4	0.648	0.729 (12.5%)	0.645 (-0.463%)	76.93	83.98 (9.16%)	76.26 (-0.87%)
	6	1.064	1.183 (11.18%)	1.054 (-0.94%)	115.9	126.1 (8.80%)	114.4 (-1.29%)
Type 3	1.5	0.054	0.068 (25.93%)	0.054 (0.00%)	13.01	13.39 (2.92%)	11.22 (-13.76%)
	2	0.102	0.122 (19.61%)	0.102 (0.00%)	18.22	18.66 (2.41%)	16.61 (-8.83%)
	4	0.287	0.324 (12.89%)	0.285 (-0.70%)	37.33	37.33 (0.00%)	34.12 (-8.60%)
	6	0.478	0.526 (10.04%)	0.464 (-2.93%)	56.06	56.02 (-0.07%)	51.17 (-8.72%)

To compare theoretical and numerical results with experimental results graphically, C_T and C_D are defined in Equation (4). C_T and C_D are called thrust and discharge similarity ratios,

respectively. These coefficients give which of the theoretical and numerical results is closer to the experimental result. The similarity ratios can be seen in Figure 9 according to nozzle types.

$$C_T = \frac{F_{theoretical\ or\ numerical}}{F_{experimental}} \quad (4)$$

$$C_D = \frac{Q_{theoretical\ or\ numerical}}{Q_{experimental}}$$

The thrust and discharge coefficients between the numerical and experimental results are generally close to 1 for all nozzle types, except for the discharge coefficient for Type 3. The discharge coefficient between the theoretical and experimental results is closer to 1 for Type 3. Consequently, the results of the numerical approach are generally closer to experimental results than those of the analytical approach.

6. Discussion and Conclusions

This study examines the effect of inlet and outlet diameters of nozzles with the same cone half angle on thrust and volumetric flow rate. Thus, it enables the selection of the nozzle with the same half-cone angle according to the inlet and outlet diameters. In this study, the convergent conical type nozzles having different inlet and exit diameters but the same cone-half angle are

investigated analytically, numerically and experimentally. According to the experimental results, the order of the thrust is as follows: Type 1 > Type 2 > Type 3. The same rankings are observed for the volumetric flow rate results. However, Type 1 results are very close to Type 2 results. Therefore, it is concluded that the increase in nozzle inlet diameter slightly decreases the thrust and volumetric flow rate only due to friction. However, the larger outlet diameter at the nozzle produces a higher thrust. As a result, it can be said that the outlet diameter affects the thrust and volumetric flow much more than the inlet diameter. For the theoretical approach, the order of the results is as follows: Type 1 = Type 2 > Type 3. According to the numerical approach, the order of the results shows that Type 1 \cong Type 2 > Type 3. According to the comparison of approaches, it can be stated that the numerical approach with ANSYS Fluent is generally more reliable than the analytical approach since it is closer to experimental results.

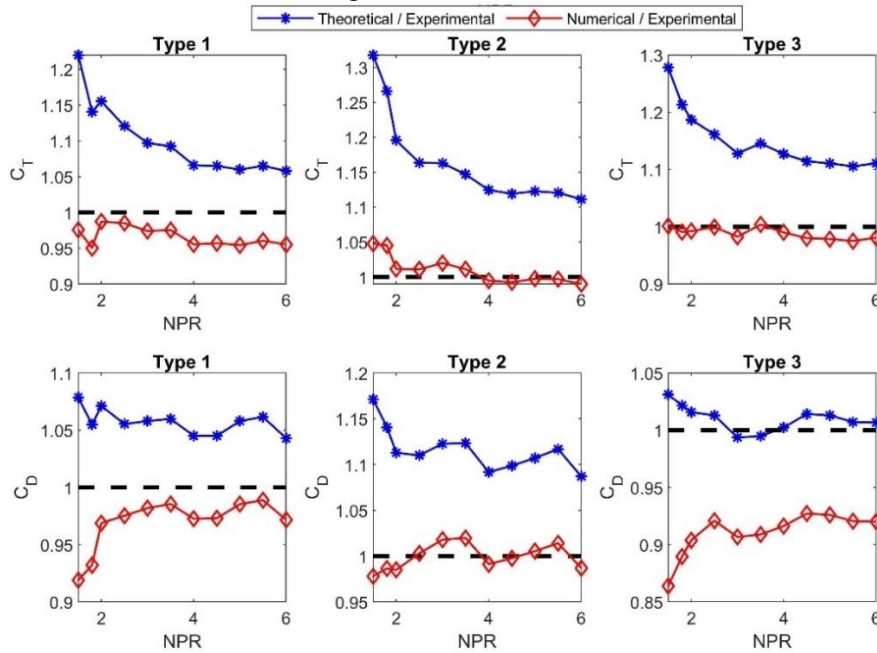


Figure 9. The similarity ratios between the results

Şekil 9. Sonuçlar arasındaki benzerlik oranları

6. Tartışma ve Sonuç

Bu çalışma, aynı koni yarım açısına sahip nozulların giriş ve çıkış çaplarının itme ve hacimsel debi üzerindeki etkisini

incelemektedir. Böylece giriş ve çıkış çaplarına göre aynı yarım koni açısına sahip nozul seçimine olanak sağlar. Bu çalışmada, farklı giriş ve çıkış çaplarına sahip fakat aynı koni-yarım

açısına sahip yakınsak konik tip nozullar analitik, sayısal ve deneysel olarak incelenmiştir. Deneysel sonuçlara göre itki sıralaması Tip 1 > Tip 2 > Tip 3 şeklindedir. Hacimsel debi sonuçlarında da aynı sıralama görülmektedir. Ancak Tip 1 sonuçları Tip 2 sonuçlarına çok yakındır. Bu nedenle, nozul giriş çapındaki artışın itme ve hacimsel debiyi sadece sürtünmeden dolayı hafifçe azalttığı sonucuna varılmıştır. Bununla birlikte, yakınsak nozuldaki daha büyük çıkış çapı, daha yüksek bir itme gücü ürettiği gözlemlenmiştir. Sonuç olarak, nozul çıkış çapının itme ve hacimsel debiyi giriş çapına göre çok daha fazla etkilediği söylenebilir. Teorik yaklaşım için sonuçların sırası şu şekildedir: Tip 1 = Tip 2 > Tip 3. Sayısal yaklaşıma göre sonuçların sıralaması Tip 1 \cong Tip 2 > Tip 3 şeklindedir. Yaklaşımlar karşılaştırıldığında, ANSYS Fluent ile sayısal yaklaşımın deneysel sonuçlara daha yakın olması nedeniyle genel olarak analitik yaklaşıma göre daha güvenilir olduğu söylenebilir.

7. Ethics committee approval and conflict of interest statement

There is no need to obtain permission from the ethics committee for the article prepared.

There is no conflict of interest with any person/institution in the article prepared.

Nomenclature

A – Cross-section area of the nozzle (m^2)

ρ – Density of fluid ($kg.m^{-3}$)

V – Velocity in x direction ($m.s^{-1}$)

P – Pressure (Pa)

h – Enthalpy ($kg.m^2.s^{-2}$)

R – Gas constant ($J.Kg^{-1}.K^{-1}$)

T – Temperature of fluid (K)

γ – Ratio of specific heats

C_v – Specific heats capacity at constant volume ($Pa.m^3.kg^{-1}.K$)

C_p – Specific heats capacity at constant pressure ($Pa.m^3.kg^{-1}.K$)

\dot{m} – Mass flow rate ($kg.s^{-1}$)

Q – Volumetric flow rate ($L.min^{-1}$)

M – Mach number

C_T – Thrust similarity ratio

C_D – Discharge similarity ratio

References

- [1] Boyanapalli, R., Vanukuri, R.S.R., Gogineni, P., Nookala, J., Yarlagadda, G.K., Gada, V. 2013. Analysis of Composite De-Laval Nozzle Suitable For Rocket Applications, International Journal of Innovative Technology and Exploring Engineering, 2, 336-344.
- [2] Dalkiran, F.Y., Toraman, M. 2020. Predicting Thrust of Aircraft Using Artificial Neural Networks. Aircraft Engineering and Aerospace Technology, 93/1 35–41. DOI: 10.1108/AEAT-05-2020-0089.
- [3] Hızarcı, B., Kiral, Z. 2019. Hava Jet İtkileri Kullanarak Mühendislik Yapılarının Aktif Titreşim Kontrolü, Konya Mühendislik Bilimleri Dergisi, 933-947. DOI: 10.36306/konjes.624373
- [4] Hızarcı, B., Kiral, Z. 2022. Experimental Investigation Of Vibration Attenuation On A Cantilever Beam Using Air-Jet Pulses With The Particle Swarm Optimized Quasi Bang-Bang Controller, Journal of Vibration and Control, 28(1-2), 58-71. DOI: doi:10.1177/1077546320971160
- [5] Dang Le, Q., Mereu, R., Besagni, G., Dossena, V., Inzoli, F. 2018. Computational Fluid Dynamics Modeling Of Flashing Flow In Convergent-Divergent Nozzle, Journal of Fluids Engineering, 140 (10). DOI: 10.1115/1.4039908
- [6] Pathan, K.A., Dabeer, P.S., Khan, S.A. 2018. Optimization of Area Ratio and Thrust in Suddenly Expanded Flow At Supersonic Mach Numbers, Case Studies In Thermal Engineering, 12, 696-700. DOI: 10.1016/j.csite.2018.09.006
- [7] Zhu, J., Elbel, S. 2020. CFD Simulation of Vortex Flashing R134a Flow Expanded Through Convergent-Divergent Nozzles, International Journal of Refrigeration, 112, 56-68. DOI: 10.1016/j.ijrefrig.2019.12.005
- [8] Thornock, R.L., Brown, E.F. 1972. An Experimental Study of Compressible Flow Through Convergent-Conical Nozzles Including a Comparison With Theoretical Results, ASME Journal of Fluids Engineering, 94, pp. 926–930. DOI: 10.1115/1.3425591
- [9] Spotts, N.G., Guzik, S., Gao, X. 2013. A CFD Analysis of Compressible Flow Through Convergent-Conical Nozzles. In 49th AIAA/ASME/SAE/ASEE Joint Propulsion Conference, July 14 - 17, 2013, San Jose, CA, 3734.
- [10] Su, C., Cheng, Y.H. 2018. Numerical and Experimental Research on Convergence Angle of Wet Sprayer Nozzle. Civil Engineering Journal, 4(9), 1985-1995.
- [11] Sun, X.L., Wang, Z.X., Zhou, L., Liu, Z.W., Shi, J.W. 2016. Influences of Design Parameters on a Double Serpentine Convergent Nozzle, Journal of Engineering for Gas Turbines and Power, 138 (7). DOI: 10.1115/1.4032338
- [12] Kumar, M., Sahoo, R.K., Behera, S.K. 2019. Design and Numerical Investigation To Visualize The Fluid Flow and Thermal Characteristics of Non-Axisymmetric Convergent Nozzle, Engineering Science and Technology, an International Journal, 22(1), 294-312. DOI: 10.1016/j.jestech.2018.10.006
- [13] Alam, M.M.A., Setoguchi, T., Matsuo, S., Kim, H.D. 2016. Nozzle Geometry Variations On The Discharge Coefficient, Propulsion and Power Research, 5(1), 22-33. DOI: 10.1016/j.jprr.2016.01.002
- [14] Payri, R., Tormos, B., Salvador, F.J., Araneo, L. 2008. Spray Droplet Velocity Characterization for Convergent Nozzles with Three Different Diameters, Fuel, 87(15-16), 3176-3182. DOI: 10.1016/j.fuel.2008.05.028
- [15] Jiang, T., Huang, Z., Li, J., Zhou, Y., Xiong, C. 2022. Effect of Nozzle Geometry on the Flow Dynamics and Resistance Inside and Outside the Cone-Straight

- Nozzle. ACS omega, 7(11), 9652-9665. DOI: 10.1021/acsomega.1c07050
- [16] Lakdawala H., Gupta A., Patel V., Jariwala H., Chaudhari G. 2022. Experimental Investigations of Jet Expansion for Hydraulic Nozzles of Different Materials, International Journal of Engineering Trends and Technology, vol. 70, no. 3, pp. 140-150. DOI: 10.14445/22315381/IJETT-V70I2P216
- [17] Kubo, K., Miyazato, Y., Matsuo, K. 2010. Study of Choked Flows Through a Convergent Nozzle. Journal of Thermal Science, 19(3), 193-197. DOI: 10.1007/s11630-010-0193-3
- [18] Martinez, I. n.d. Nozzles. <http://imartinez.etsiae.upm.es/~isidoro/bk3/c17/Nozzles.pdf>. (Retrieved March 22, 2021).
- [19] Yaravintelimath, A., Raghunandan, B.N., Moríño, J.A. 2016. Numerical Prediction of Nozzle Flow Separation: Issue of Turbulence Modeling, Aerospace Science and Technology, 50, 31-43. DOI: 10.1016/j.ast.2015.12.016
- [20] Elmekawy, A.M.N. n.d. SPC 407 Supersonic & Hypersonic Fluid Dynamics Ansys Fluent Tutorial 4 Compressible Flow through Convergent Conical Nozzle. https://drahmednagib.com/onewebmedia/SPC407/Fluent_Tutorial_Conical_Convergent_Nozzle.pdf (Retrieved July 05, 2022).
- [21] SMC Nozzle datasheet. n.d., Blow Gun. https://static.smc.eu/pdf/VMG-F_EU.pdf. (Retrieved November 15, 2022).
- [22] NASA. n.d. Grids - Axisymmetric Subsonic Jet Case. https://turbmodels.larc.nasa.gov/jetsubsonic_grids.html (Retrieved July 05, 2022).
- [23] Fluent, ANSYS. 2013. Ansys Fluent Theory Guide. <https://www.afs.enea.it/project/neptunius/docs/fluent/html/ug/node167.htm> (Retrieved July 05, 2022).
- [24] NASA. n.d. ASJ: Axisymmetric Subsonic Jet. https://turbmodels.larc.nasa.gov/jetsubsonic_val.html (Retrieved November 15, 2022).